



Unsteady Ejector Performance: An Experimental Investigation Using a Pulsejet Driver

Daniel E. Paxson
Glenn Research Center, Cleveland, Ohio

Jack Wilson and Kevin T. Dougherty
QSS Group, Inc., Cleveland, Ohio

The NASA STI Program Office . . . in Profile

Since its founding, NASA has been dedicated to the advancement of aeronautics and space science. The NASA Scientific and Technical Information (STI) Program Office plays a key part in helping NASA maintain this important role.

The NASA STI Program Office is operated by Langley Research Center, the Lead Center for NASA's scientific and technical information. The NASA STI Program Office provides access to the NASA STI Database, the largest collection of aeronautical and space science STI in the world. The Program Office is also NASA's institutional mechanism for disseminating the results of its research and development activities. These results are published by NASA in the NASA STI Report Series, which includes the following report types:

- **TECHNICAL PUBLICATION.** Reports of completed research or a major significant phase of research that present the results of NASA programs and include extensive data or theoretical analysis. Includes compilations of significant scientific and technical data and information deemed to be of continuing reference value. NASA's counterpart of peer-reviewed formal professional papers but has less stringent limitations on manuscript length and extent of graphic presentations.
- **TECHNICAL MEMORANDUM.** Scientific and technical findings that are preliminary or of specialized interest, e.g., quick release reports, working papers, and bibliographies that contain minimal annotation. Does not contain extensive analysis.
- **CONTRACTOR REPORT.** Scientific and technical findings by NASA-sponsored contractors and grantees.

- **CONFERENCE PUBLICATION.** Collected papers from scientific and technical conferences, symposia, seminars, or other meetings sponsored or cosponsored by NASA.
- **SPECIAL PUBLICATION.** Scientific, technical, or historical information from NASA programs, projects, and missions, often concerned with subjects having substantial public interest.
- **TECHNICAL TRANSLATION.** English-language translations of foreign scientific and technical material pertinent to NASA's mission.

Specialized services that complement the STI Program Office's diverse offerings include creating custom thesauri, building customized data bases, organizing and publishing research results . . . even providing videos.

For more information about the NASA STI Program Office, see the following:

- Access the NASA STI Program Home Page at <http://www.sti.nasa.gov>
- E-mail your question via the Internet to help@sti.nasa.gov
- Fax your question to the NASA Access Help Desk at 301-621-0134
- Telephone the NASA Access Help Desk at 301-621-0390
- Write to:
NASA Access Help Desk
NASA Center for Aerospace Information
7121 Standard Drive
Hanover, MD 21076



Unsteady Ejector Performance: An Experimental Investigation Using a Pulsejet Driver

Daniel E. Paxson
Glenn Research Center, Cleveland, Ohio

Jack Wilson and Kevin T. Dougherty
QSS Group, Inc., Cleveland, Ohio

Prepared for the
38th Joint Propulsion Meeting and Exhibit
cosponsored by AIAA, ASME, SAE, and ASEE
Indianapolis, Indiana, July 7-10, 2002

National Aeronautics and
Space Administration

Glenn Research Center

This report is a formal draft or working paper, intended to solicit comments and ideas from a technical peer group.

This report contains preliminary findings, subject to revision as analysis proceeds.

The Aerospace Propulsion and Power Program at NASA Glenn Research Center sponsored this work.

Available from

NASA Center for Aerospace Information
7121 Standard Drive
Hanover, MD 21076

National Technical Information Service
5285 Port Royal Road
Springfield, VA 22100

Available electronically at <http://gltrs.grc.nasa.gov/GLTRS>

UNSTEADY EJECTOR PERFORMANCE: AN EXPERIMENTAL INVESTIGATION USING A PULSEJET DRIVER

Daniel E. Paxson[†]
National Aeronautics and Space Administration
Glenn Research Center
Cleveland, Ohio 44135, USA
Phone: 216-433-8334
FAX: 216-433-8643
Email: Daniel.E.Paxson@grc.nasa.gov

Jack Wilson[‡]
QSS Group Inc.
Cleveland, Ohio 44135, USA
Phone: 216-977-1204
FAX: 216-977-1334
Email: Jack.Wilson@qssgess.com

Kevin T. Dougherty[†]
QSS Group Inc.
Cleveland, Ohio 44135, USA
Phone: 216-433-3546
FAX: 216-433-2182
Email: Kevin.T.Dougherty@grc.nasa.gov

Abstract

An experimental investigation is described in which thrust augmentation and mass entrainment were measured for a variety of simple cylindrical ejectors driven by a gasoline-fueled pulsejet. The ejectors were of varying length, diameter, and inlet radius. Measurements were also taken to determine the effect on performance of the distance between pulsejet exit and ejector inlet. Limited tests were also conducted to determine the effect of driver cross-sectional shape. Optimal values were found for all three ejector parameters with respect to thrust augmentation. This was not the case with mass entrainment, which increased monotonically with ejector diameter. Thus, it was found that thrust augmentation is not necessarily directly related to mass entrainment, as is often supposed for ejectors. Peak thrust augmentation values of 1.8 were obtained. Peak mass entrainment values of 30 times the driver mass flow were also observed. Details of the experimental setup and results are presented. Preliminary analysis of the results indicates that the enhanced performance obtained with an unsteady jet (primary source) over comparably sized ejectors driven with steady jets is due primarily to the structure of the starting vortex-type flow associated with the former.

Introduction

Unsteady ejectors are currently under investigation for use in some Pulse Detonation Engine (PDE) propulsion

systems. This is due in part to their potentially high performance compared to steady ejectors of the same size relative to the jet dimensions.^{1,2,3} Additionally, they may help to reduce noise and high levels of unsteadiness in the exhaust flow, both of which are features of PDE's. The performance referred to here is the so-called thrust augmentation of the ejector, ϕ defined as

$$\phi \equiv \frac{T^{\text{Total}}}{T^{\text{j}}} \quad (1)$$

where T^{Total} is the total thrust of the combined ejector and primary (i.e. driving) jet and T^{j} is the thrust due to the primary jet alone. In this definition, the primary jet thrust is often defined as being that obtained with no ejector present. It has been argued that the presence of an ejector lowers the jet exit pressure, thereby increasing its thrust and contributing to an increased total thrust. For most of the jets considered in this paper however, the difference between jet exit plane pressure and that of the ambient air is small. Thus, installed jet thrust measurements are sufficiently accurate.

Thrust augmentation values as high as 2.0–2.4 have been reported using a single pulsed primary jet and ejectors of remarkably small, simple design.¹ While state-of-the-art ejectors driven by steady jets can

[†] Senior Member AIAA

[‡] Associate Fellow, AIAA

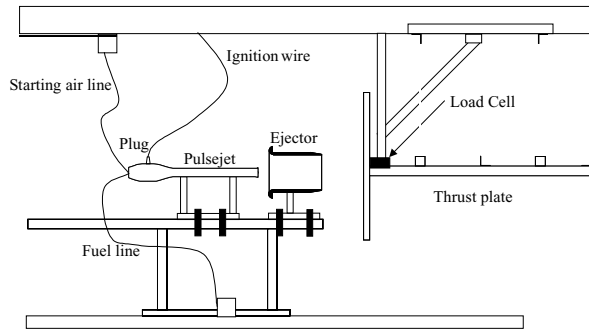


Fig. 1 Experimental setup for measuring thrust augmentation.

achieve similar steady performance, they require multiple jets and large, long ejector bodies.³

Unfortunately, no proven theory of unsteady ejector performance appears to exist in the literature. Perhaps for this reason, neither does a consistent set of design criteria or scaling laws that would allow the construction of an effective ejector for an arbitrary pulsed flow. In order to provide this sort of information, an experimental facility has been constructed at the NASA Glenn Research Center. A commercially available pulsejet⁴ design was used for the primary unsteady jet. This was paired with a basic, yet flexible ejector that allowed parametric evaluation of the effects that length, diameter, and inlet radius have on performance.

The use of a pulsejet is advantageous in several ways. First, pulsejets are mechanically (though not fluid dynamically) simple, and they are inexpensive to build and operate, particularly when compared to the target ejector application, PDE's. These features allowed for rapid build-up and subsequent data acquisition. Second, since the end goal of the investigation is in application to PDE's, it is beneficial to use a primary jet that closely resembles them. The pulsejet does so in that the exiting flow has very high enthalpy compared to the secondary flow being entrained, the fluctuations in exit velocity are very large with complete flow reversal occurring over part of the cycle. Furthermore, the 220 hz. frequency of the particular unit used in this experiment is similar those of PDE's being considered for flight. Since all three of these similarities (i.e. primary enthalpy, jet impulse shape, and frequency) may influence the performance of pulsed ejectors, it may be possible to extrapolate the results obtained in this experiment to actual PDE's. It is noted however, that pulsejet exhaust flows differ substantially from those of PDE's in that the latter have strong associated gasdynamic waves that pulsejets do not. These waves may substantially impact the performance of ejectors.

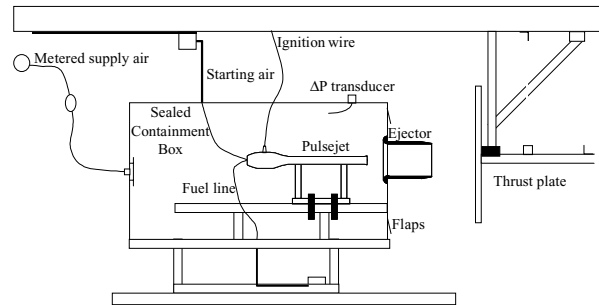


Fig. 2 Experimental setup for measuring entrainment.

This paper describes the experimental setup, operation, and data acquisition methods of the Glenn facility. Results obtained to date are also presented. Analysis of these results, and comparison with other experiments^{3,5} indicates that the particular shape (i.e. time history) of the exiting jet flow, along with its associated starting vortex is primarily responsible for the enhanced performance over steady ejectors observed here and elsewhere.¹⁻⁵ The manner in which this jet entrains secondary flow determines thrust augmentation. This indication suggests that, in the absence of a well-defined theory, predictions of unsteady ejector performance should have a correlation parameter that characterizes the exiting jet flow. Such a parameter is discussed herein.

Experimental Setup

Two configurations were used in the experiment. One was used for measuring thrust augmentation. The other was used to measure ejector mass entrainment. They are shown schematically in Figs. 1 and 2, respectively and are described below.

Thrust Augmentation Rig

The open rig used ambient air to supply the pulsejet and ejector. The pulsejet and ejector(s) were each mounted on stands that were in turn clamped to a fixed rail. This configuration allowed variations of the distance between the pulsejet and the ejector as well as between the ejector and the thrust plate. Of course, it was also possible to remove the ejector entirely and measure the thrust of the pulsejet alone.

Thrust Plate

The thrust plate was 2.0 ft. square in dimensions. It was attached to a frame and ultimately suspended from a beam in the ceiling of the test cell by four chains as shown in Fig. 1. A load cell was attached to a fixed mount and placed at the center of the thrust plate. The axial position of the load cell was adjusted so as to

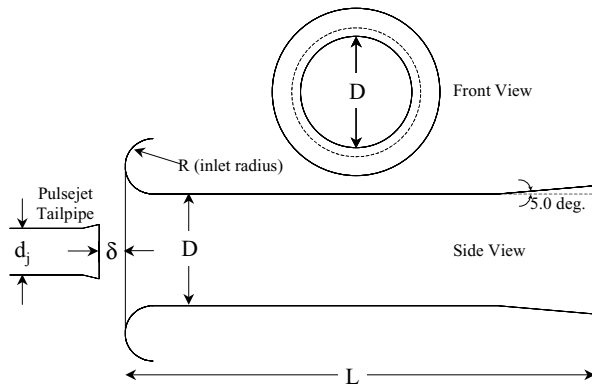


Fig. 3 Ejector design and parametric variables.

create a small amount of preload (i.e. it pushed the thrust plate forward from the neutral hanging position).

A small pad of silicone was placed between the load cell and the thrust plate in order to reduce vibrations. Furthermore, stiffeners were added to the thrust plate and the load cell mount. Nevertheless, the signal from the load cell was far from steady. The frequency content was dominated by the 220 hz. signal of the pulsejet and an approximately 14 hz. natural frequency of the plate. It was therefore coupled to a 1 hz. low-pass filter. Furthermore, the filtered signal was read from an averaging circuit on an oscilloscope with a sweep period of 5.0 seconds.

The distance between the thrust plate and either the pulsejet or ejector was found to make little difference to the readings obtained. This was an expected result and held true provided the plate was not so close as to alter the back pressure of the jet (approximately one diameter), or so far as to become smaller in dimension than the jet plume. In the present tests, the distance varied between 15 diameters for the pulsejet alone, to 2.5 for the largest ejector.

Mass Entrainment Rig

In the entrainment rig, the pulsejet and ejector were placed within a sealed containment box. Originally, the only openings in the box were those made for the ejector exhaust and for a metered supply line. It was found however that the pulsejet, which has a Venturi fuel feed system, and which was installed with the fuel reservoir outside the containment box, was operationally sensitive to the pressure in the box. If significant air flow was established through the containment box prior to starting the pulsejet, the pressure inside would rise relative to the ambient pressure. This, in turn, would starve the pulsejet of fuel (i.e. the venturi system could not overcome the pressure

differential). On the other hand, if the pulsejet was started prior to flowing air through the box, the ejector would immediately begin acting as a pump. This would quickly lower the pressure in the containment box relative to ambient pressure and essentially flood the pulsejet. The solution to the problem was to install a set of four flap valves in back of the containment box. The valves were simply 3.0 in. diameter holes covered on the outside with a piece of hinged plastic sheet. The hinge (actually tape) was placed at the top of the sheet. Thus, if the pressure in the box rose above ambient, they would open. At ambient pressure, or below, they would close.

With this arrangement, it was possible to establish airflow through the box first, and subsequently start the pulsejet. Due to thermal considerations, the pulsejet was only operated for 15 sec. per run. During this time, a highly sensitive (i.e. ± 7.5 in. H_2O) differential pressure transducer in the containment box was monitored. If the reading was below ambient, then the mass flow to the box was increased for the next run. If it was above ambient, mass flow was decreased. In this trial and error manner, airflow into the box was adjusted until the pressure in the box was equal to the ambient pressure.

Ejectors

The series of ejectors examined were essentially of a straight, cylindrical form, although a small divergence was added at the exhaust ends.⁵ An example is shown in Fig. 3, along with the parametric designations used elsewhere in the paper. The variable parameters were the length, L , the diameter, D and the rounding radius on the inlet, R . It was also possible to measure the effect of the spacing between pulsejet exhaust and ejector inlet, δ . For all of the ejectors tested, the length of the divergent section was the same (2.625 in.). The pulsejet diameter d_j was 1.25 in.

Pulsejet Primary Source

As described earlier, the unsteady flow source was a gasoline-fueled pulsejet shown in Fig. 4. The operational theory of these resonant devices can be found in numerous sources and will not be presented here.^{1,4} The design was that of the commercially available Dynajet model. In fact, the valve body and valve were obtained directly from a Dynajet pulsejet. The combustion chamber and tailpiece were machined from Inconel according to Dynajet specified dimensions. The exception to this was the wall thickness, which was approximately doubled. Since the pulsejet was run statically in the experiment, there was no convective cooling available. This meant that the material became particularly hot, and was the reason

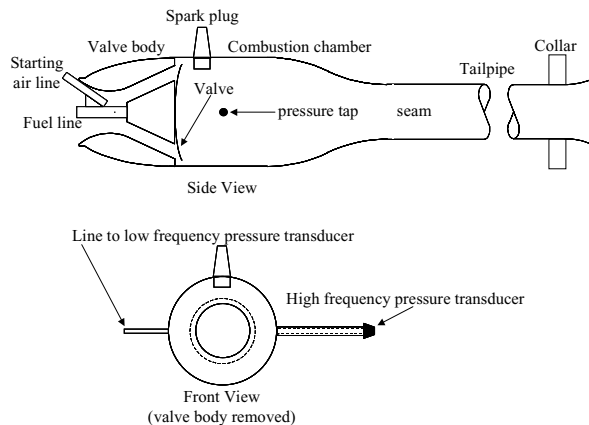


Fig. 4 Pulsejet primary unsteady jet source.

that test durations were limited to 15 sec. The commercially produced Dynajet was made from thin (0.015 in.) stainless steel and was constructed from two half-shells requiring two full-length seam-welds. Even with the short tests, the welded seam tended to rupture after only a few runs. The use of high temperature materials (Inconel) and machining to create a pulsejet with only one circumferential seam resulted in an almost indefinite operational life.

The pulsejet was instrumented with two static pressure transducers. One was a low frequency, remotely located type, connected to the pulsejet by several feet of 0.0625 in. OD tubing. The other was a high frequency, high temperature (750 °F) transducer mounted to a 0.125 in. ID standoff tube, 2.5 in. in length. Figure 5 shows a sample trace from the high frequency transducer during operation. The ambient pressure has been subtracted. Also shown in the figure are the average value of the trace (over the 0.2 sec. interval) and the average value of the low frequency transducer read from an averaging circuit on an oscilloscope with a 5.0 second sweep. The nominal 220 hz. operating frequency can be observed in the oscillating pressure signal. It can also be seen that the average values of the high and low frequency transducers differed slightly (3.3 vs. 3.8 psig, respectively). This difference was not observed in steady-state pressure tests of the combustion chamber and is believed to be due to flowfield asymmetries during operation.

It is noted that if the mean of these two averaged pressure differences is multiplied by the area of the pulsejet tailpipe (1.227 in.²), the resulting thrust estimate is 4.36 lb_f. The value measured from the thrust plate for this particular run was 4.33 lb_f. This is an

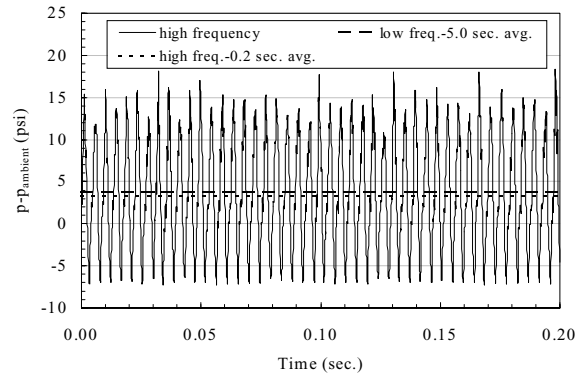


Fig. 5 Pressure trace and average pressures in the pulsejet combustion chamber during operation.

expected result and proved true over the very limited throttling range of the pulsejet. However, for unknown reasons it also proved to have significant run-to-run scatter. That is to say, on any given run, the two measurements could differ by as much as $\pm 5\%$. If an average of three runs was used, the maximum difference was only $\pm 3\%$ with a standard deviation for all of the runs of only 1.4%. Thus, for all results to be shown a three runs averaging technique was applied. Using a three run average also reduced the relatively large scatter due to natural variations in pulsejet thrust.

By calculating thrust from the combustion chamber pressures, it was possible to measure the pulsejet thrust while it was coupled with an ejector. This capability is important since, as will be shown hence, some ejector configurations had a rather large effect on pulsejet operation and therefore on the thrust produced. Since this effect is not likely to occur with other unsteady sources, such as PDE's, it has been eliminated from the most of the results presented (i.e. by using in-situ primary thrust).

Tailpieces

For the majority of tests conducted, the final approximately three inches of the pulsejet were as shown in Fig. 4. That is, the tailpipe was flared and a collar was permanently attached for installation in the containment box without ejectors (i.e. for measuring mass flow through the pulsejet alone). This section will be designated as the tailpiece, and the particular arrangement in Fig. 4 will be designated ORIGINAL. In an effort to examine the effect of the jet shape, the pulsejet was actually constructed such that different tailpieces could be threaded on to the same tailpipe. Limited tests were conducted on three other configurations. These are shown in Fig. 6 along with their designations. It is noted that the STAR tailpiece

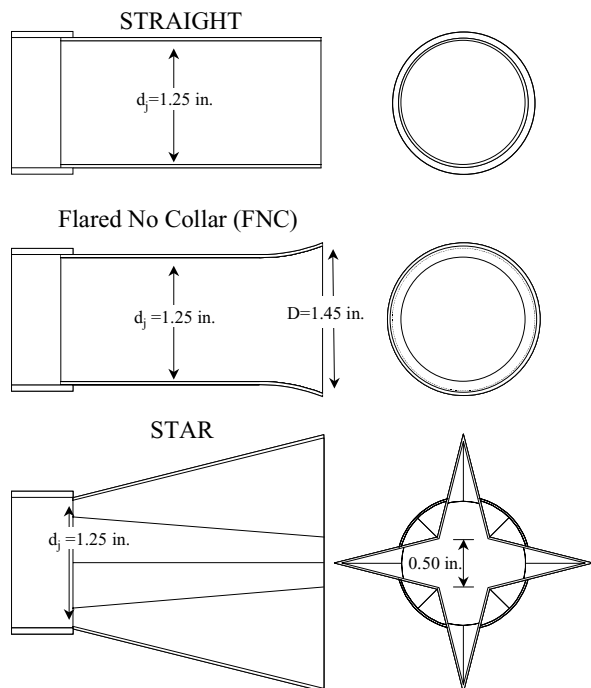


Fig. 6 Various tested tailpiece configurations for the final approximately 3.0 inches of the pulsejet tailpipe.

had the same cross sectional area as the STRAIGHT tailpiece along its entire length.

Results: Thrust Augmentation

Ejector Length

The effects of ejector length on thrust augmentation are shown in Fig. 7 for various ejector diameters. For all of the data in this figure the spacing between pulsejet exit and ejector inlet was maintained at a constant value of $\delta/d_j=2.0$. The figure shows thrust augmentation plotted two ways. The first is in the conventional manner, with the pulsejet thrust being defined as that obtained without an ejector present. The second method, designated 'insitu' uses the pulsejet thrust measured with the ejector present, using the pressure in the combustion chamber as described earlier in the paper. For both methods the total thrust is the same value, obtained from the thrust plate. Although the two methods do not differ substantially in their resultant values at this particular δ/d_j location, they do at others (see Fig. 8). More importantly however, they differ in terms of trends. Both show clear maxima for the $D=3.0$ and 4.0 in. ejectors; however, for the 'insitu' measurements, both the $D=2.2$ and 6.0 in. ejectors show continuously increasing augmentation with larger L , while the conventional measurements show weak maxima.

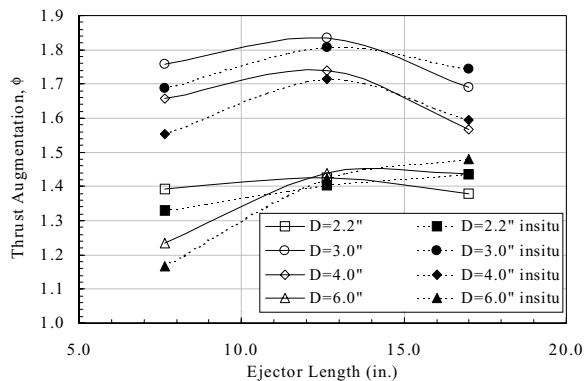


Fig. 7 Thrust augmentation as a function of ejector length for various ejector diameters, with fixed $\delta/d_j=2.0$ and $R=0.75$ in.

Because the pulsejet is a resonant device, its performance is quite sensitive to, among other things, exit pressure. Thus, the presence of ejectors can strongly influence the thrust delivered. As mentioned earlier, this behavior is believed to be unique to pulsejets (and possibly other resonant, unsteady thrust sources⁵) and therefore not applicable to forced unsteady devices such as PDE's. Furthermore, it is the performance of the ejector that is of interest here, and not the thrust source. Thus, unless otherwise stated, the 'insitu' thrust augmentation measurement will be used.

Examination of Fig. 7 reveals two interesting trends. The first is that the maxima for the $D=3.0$ and 4.0 in., and arguably, at least a 'knee' in the $D=2.2$ and 6.0 in. ejectors all occur at the same length. This suggests that scaling for optimal length should not be based on some number of ejector diameters, as is typically done with steady ejectors, but instead should be based on some parameter of the unsteady jet flow. This argument is further substantiated by the observation that Refs. 1, 2 and 5 all showed different values of L/D for which peak performance occurred. The second evident trend in Fig. 7 is the presence of a clear ejector diameter at which peak performance occurs. The $D=3.0$ ejector shows superior performance at all lengths over the other diameters. Taking the ratio of this diameter to the pulsejet (driver) diameter gives a value of $D/d_j=2.4$. This is similar to the peak values observed in Refs. 1 and 5 of 3.3 and 3.0 respectively. This was also near the value used in Ref. 2, although it is not certain that this was optimal. It is noted that the jet driver in Ref. 5 is annular, and d_j was taken to be the hydraulic diameter. These results suggest that for unsteady ejectors of the cylindrical type, scaling diameters for peak performance may be geometrically related to the primary jet source diameter.

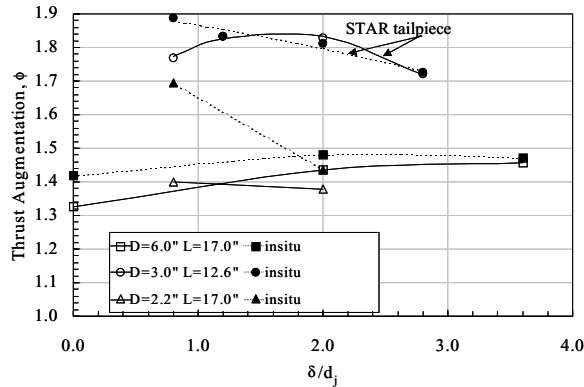


Fig. 8 Thrust augmentation as a function of distance between pulsejet exhaust and ejector inlet for several ejector diameters, with $R=0.75$ in.

Ejector Proximity

The effect of spacing between primary jet and ejector inlet is shown in Fig. 8 for several different values of D . For each diameter shown, the ejector length was that which gave the best performance at $\delta/d_j=2.0$. In the present experiment, the 3.0 in. diameter ejector yielded the best performance for any of the lengths tested. Unfortunately, for the optimal length at this diameter ($L=12.6$ in.) proximity data was only obtained with the STAR tailpiece shown in Fig. 6. The other proximity data was obtained with the ORIGINAL tailpiece; however, it is not expected that the tailpiece shape will alter the trends shown in Fig. 8. For all of the data shown in this figure the inlet radius was $R=0.75$ in. The figure also shows both conventional and insitu augmentation results in order to underscore the substantial effect of the ejector on pulsejet performance.

Examining the conventionally measured augmentation data, it can be seen that for the $D=3.0$ in. ejector peak performance occurs at approximately 1.8 jet diameters. For the $D=6.0$ in. ejector, the peak appears to occur at $\delta/d_j=2.0$; however, this is no definitive. Similarly, for $D=2.2$ in., the peak must be estimated, and appears to occur near $\delta/d_j=0.0$. This trend (δ/d_j decreasing with D) is consistent with the results of Ref. 5. If insitu thrust augmentation is examined however, the results are quite different. Here it is seen that, although the $D=6.0$ in. ejector shows a peak, both the $D=3.0$ and 2.2 in. ejectors show increased augmentation as the primary jet moves toward the ejector. It is not known whether a peak occurs somewhere inside the ejector. Unfortunately, the leftmost points of Fig. 8 (for $D=3.0$ and 2.2 in.) were the smallest values of δ/d_j for which the pulsejet could successfully be started. Noting again that PDE's will not likely suffer the same performance

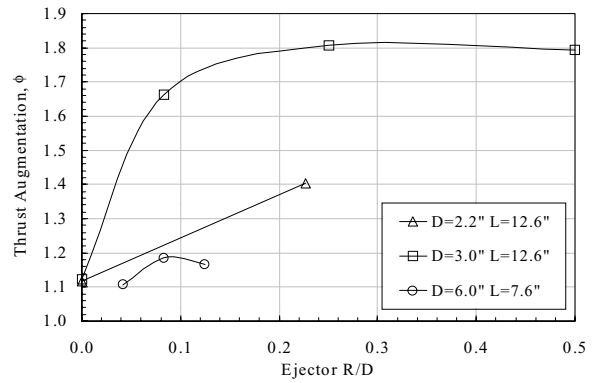


Fig. 9 Thrust augmentation as a function of ejector inlet rounding for various ejector diameters and lengths, with fixed $\delta/d_j=2.0$.

effects as pulsejets due to ejector proximity, Fig. 8 suggests that improved performance can be gained by placing the primary jet inside the ejector inlet.

Ejector Inlet Rounding

Figure 9 illustrates the dependence of thrust augmentation on the inlet rounding, R for several ejector diameters. The ejector length was only optimal for the $D=3.0$ in. ejector (an unfortunate mistake); however, since this was clearly the diameter yielding the best performance, the results are still useful. For the results in this figure the value of δ/d_j was 2.0. Data at $R/D=0.0$ was obtained, for the $D=3.0$ in. case, using 3.25 in. diameter sheet metal tubing (stove pipe). Thus, the specified ejector diameter should be interpreted as nominal. For the $D=2.2$ in. case, data at $R/D=0.0$ was obtained by reversing the ejector and removing the rounded inlet. Obviously, for different values of R the length of the ejectors changes. The change is small however, and insignificant to the results.

The effects of inlet rounding are quite striking for the $D=3.0$ in. ejector, particularly in contrast to the Ref. 5 experiment which, using the same ejectors, showed virtually no effect on performance. It is not clear why this would be so; however, it may suggest that it is related to the nature of the jet, which differed markedly between the two experiments. It may also suggest that the effect of lip rounding depends on the overall performance of the ejector. It can be seen that the effects were quite small for the $D=6.0$ in. ejector, but so was the augmentation level. The Ref. 5 experiment also had fairly low levels of augmentation. It does not appear that ejector diameter is the proper length scale for the inlet rounding since, at different diameters the peak performance in Fig. 9 occurred at different values of R/D . The appropriate length scale is not clear at this

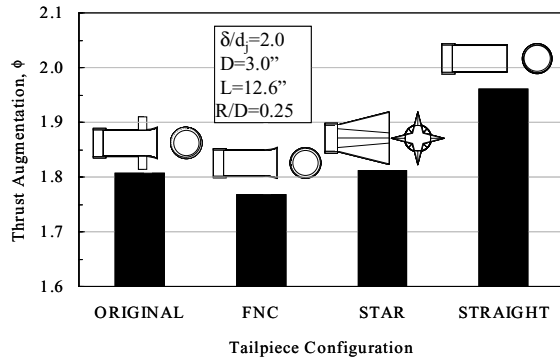


Fig. 10 Thrust augmentation for various tailpiece configurations using the $D=3.0$, $L=12.6$, $R/D=0.25$ ejector at $\delta/d_j=2.0$.

time. It can also be seen that there is a point at which further increases in rounding do not yield improved performance.

Jet Tailpiece Profiles

Limited testing was performed with the different tailpieces shown in Fig. 6. The results are summarized in Fig. 10 which shows thrust augmentation for each tailpiece using the $D=3.0$, $L=12.6$, $R/D=0.25$ ejector (the configuration producing the highest thrust augmentation) at $\delta/d_j=2.0$. A significant performance difference was observed only with the STRAIGHT configuration. It is noted however that both the STAR and STRAIGHT configurations resulted in reduced pulsejet thrust compared to the ORIGINAL, even with no ejector present. This was accompanied by a slight rise in operating frequency from 220 to 238 hz. Thus, it is not clear whether improved augmentation resulted from a change in the tailpiece geometry, or a change in the nature of pulsed jet.

Results: Entrainment

Four different ejector diameters were tested in the entrainment rig shown in Fig. 2. All four had $L=12.6$ in., $R=0.75$ in., and $\delta/d_j=2.0$. Since insitu mass flow rates could not be measured in the pulsejet, the value of δ/d_j was chosen so that the performance of the pulsejet was largely unaffected by the presence of the ejector. Thus, mass flow rates were measured with the pulsejet alone and with ejectors in place. From these measurements the entrainment ratio could be calculated. This is defined as

$$\beta = \frac{\dot{m}_{\text{ejector}}}{\dot{m}_{\text{pulsejet}}} \quad (2)$$

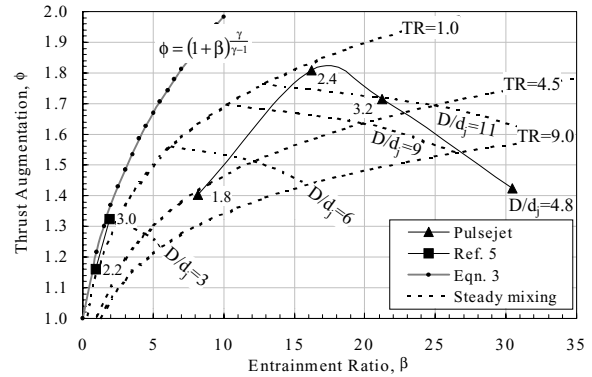


Fig. 11 Thrust augmentation as a function of entrainment ratio for various ejector diameters, with fixed $L=12.6$ in., $R=0.75$ in., and $\delta/d_j=2.0$.

where \dot{m}_{ejector} is the secondary air mass flow rate through the ejector, and $\dot{m}_{\text{pulsejet}}$ is the mass flow rate through the pulsejet alone. The value of \dot{m}_{ejector} is found by subtracting pulsejet flow from the total flow. For the tests conducted, the mean value of the pulsejet mass flow rate was $\dot{m}_{\text{pulsejet}}=0.057$ lb_m/s. Unless otherwise noted, all quantities are time-averaged.

The test results are shown in Fig. 11 where thrust augmentation is plotted as a function of entrainment ratio. The value of D/d_j is shown next to each point. Also shown in the figure are the measured results from Ref. 5 (where jet hydraulic diameter has again been used in D/d_j). A curve defined by

$$\phi = (1 + \beta)^{\frac{\gamma}{\gamma-1}} \quad (3)$$

has also been plotted. This is an empirical curve-fit for steady ejectors representing an observed limit to ejector performance,³ however, it is similar in form to the ideal limit,⁶ in which the exponent $\gamma/(\gamma-1)$ is replaced by $1/2$. Thus, the exponent may be thought of as containing an efficiency of the form $\eta_m/2$.

The results of steady, constant area mixing calculations⁷ are also shown in Fig. 11. It may be shown that for subsonic primary jets, these calculations yield thrust augmentation and entrainment ratio that depend only on the total temperature ratio and area ratio. The total temperature ratio is defined as

$$TR = \frac{\theta_{\text{jet}}^0}{\theta_{\text{secondary}}^0} \quad (4)$$

Table 1 RMS velocity values for the present and Ref. 5 experiments.

	Pulsejet	Ref. 5 (Resonance Tube)
$\sqrt{u'^2}/\bar{u}$	1.89	0.94

where θ has been used to denote temperature. Mixing calculations yield thrust augmentation values that agree very well with steady, single nozzle ejector measurements^{2,3} provided the ejectors are sufficiently long such that complete mixing can occur.

Examination of Fig. 11 reveals several interesting trends. First, the performance of the pulsejet-driven ejector is not monotonically related to entrainment ratio, an assumption often made (or implied) by other researchers.^{8,9} In fact, the ejector with the lowest thrust augmentation yielded the highest entrainment ratio.* Second, though the pulsejet primary produced much higher thrust augmentation levels, with the same ejectors, than the resonance-tube primary of Ref. 5, the efficiency of the process was, apparently much lower. Third, the entrainment ratio for all of the ejectors tested was well above that estimated for comparably sized steady ejectors. For comparison, it is noted that the measured pulsejet temperature ratio, TR was approximately 4.6 based on simple time averaging. This compares favorably with values found in the literature.¹⁰ The mass averaged temperature ratio is expected to be considerably higher, near 6.0.†

Discussion

In order to interpret some of the results presented, it may be worthwhile to consider the pulsejet thrust source as composed of two components, one steady and the other unsteady. For subsonic jets, the average thrust may be written approximately as

$$\bar{T}^j = \frac{A}{\tau g_c} \int_0^\tau \rho u^2 dt \quad (5)$$

* The entrainment ratio for $D/d_j=4.8$ was actually an extrapolated value because the facility could not supply a sufficient mass flow of air for this ejector. The extrapolation has a high level of confidence however, and is described in Appendix 1.

† This value was obtained by simulating the pulsejet cycle with a Q-1-D code¹¹ and matching mass flow, thrust and time averaged exit temperature.

where τ is the cycle period, A is the cross sectional area and g_c is the Newton constant. Although density is clearly not constant in a pulsejet, for algebraic simplicity, it will be assumed so here. Thus, denoting steady (time-averaged) and unsteady velocity components such that $u = \bar{u} + u'$, Eq. 5 may be written as

$$\bar{T}^j = \left(\frac{\rho A}{g_c} \right) \bar{u}^2 + \left(\frac{\rho A}{g_c} \right) \overline{u'^2} \quad (6)$$

where $\overline{u'^2} = \frac{1}{\tau} \int_0^\tau u'^2 dt$. The terms on the right of Eq. 6

will be denoted \bar{T}_{ss}^j , and \bar{T}_{us}^j respectively. Thus, the steady and unsteady thrust components are clearly delineated. If it is now supposed that the total thrust has similar steady and unsteady components, the following relationship may be written

$$\phi = \frac{\phi_{ss} + \frac{\overline{u'^2}}{\bar{u}^2} \phi_{us}}{1 + \frac{\overline{u'^2}}{\bar{u}^2}} \quad (7)$$

where $\phi_{ss} = \frac{\bar{T}_{ss}^{\text{Total}}}{\bar{T}_{ss}^j}$ and $\phi_{us} = \frac{\bar{T}_{us}^{\text{Total}}}{\bar{T}_{us}^j}$. Equation 7 clearly shows that the 'shape' of the unsteady primary jet, which is characterized by $\overline{u'^2}/\bar{u}^2$, plays a large role in performance.

The entrainment may also be divided into components

$$\beta = \frac{\bar{m}_{ss}^{\text{ejector}}}{\bar{m}^j} + \frac{\bar{m}_{us}^{\text{ejector}}}{\bar{m}^j} \equiv \beta_{ss} + \beta_{us} \quad (8)$$

Experimentally, the rms velocity fluctuations may be found by assuming a mean density and rearranging Eqn. 6 to read

$$\frac{\sqrt{\overline{u'^2}}}{\bar{u}} = \left\{ T^j \left(\frac{\rho A g_c}{\bar{m}^j} \right) - 1 \right\}^{1/2} \quad (9)$$

Table 1 lists these values for the present and Ref. 5 experiments. The mean density used for the present experiment in Eq. (9) was $0.0126 \text{ lb}_m/\text{ft}^3$. This value was obtained by dividing the density of standard air by the estimated mass-averaged pulsejet exhaust temperature ratio of 6.0. The result agreed well with measured rms velocity values obtained experimentally.¹² For the Ref. 5 experiment the

Table 2 Steady and unsteady augmentation and entrainment ratio components for the present and Ref. 5 experiments

D/d_j	ϕ_{ss}	β_{ss}	ϕ_{us}	β_{us}
Pulsejet Driven Ejector				
1.8	1.05	1.34	1.50	6.83
2.4	1.16	3.24	1.99	13.00
3.2	1.26	5.62	1.84	15.57
4.8	1.40	10.38	1.43	20.09
Ref. 5 Resonance Tube Driven Experiment				
2.2	1.01	0.13	1.33	0.77
3.0	1.12	0.73	1.56	1.16
4.0	1.22	-----	1.32	-----
6.0	1.36	-----	1.13	-----

standard air density of 0.076 lb_m/ft³ was used. Evidently, the unsteady thrust component of the pulsejet experiment is over three times larger than the steady component. In the resonance tube, the unsteady component is slightly less than the steady component.

Assuming that the steady-state behavior of the ejector flowfield can be modeled using the mixing calculation described earlier (though it is clear that several of the ejectors tested are far too short when scaled by the diameter), the unsteady quantities can be obtained. These are listed in Table 2. For the Ref. 5 data, the values of L and R used are those yielding the highest thrust augmentation ratios. The hydraulic diameter was used for d_j .

Figure 12 shows the unsteady thrust augmentation from the two experiments plotted as a function of ejector to jet diameter ratio. It is evident that there is a strong maximum in the vicinity of $D/d_j=3$ for both experiments, as mentioned earlier. It is well known that an impulsively started flow emitted from a pipe forms a starting vortex. It has been shown that the features of this flow change radically based on the so-called Formation number¹³

$$F = \frac{U\tau}{d_j} \quad (10)$$

where U is some characteristic velocity of the pulse and τ is a characteristic time over which the pulse occurs. Remarkably however, the maximum size of the vortex seems to scale with the dimensions of the jet. This observation is consistent with the findings here. It suggests that, for unsteady thrust augmentation, the dimensions of the ejector yielding peak performance are related to the size of the starting vortex, which in turn is

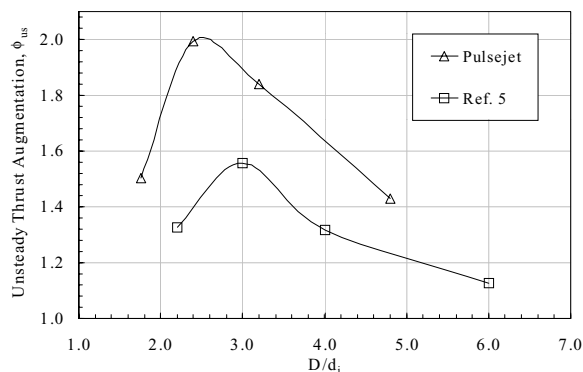


Fig. 12 Unsteady thrust augmentation as a function ejector to jet ratio for the pulsejet and Ref. 5 experiment.

Table 3 RMS velocity values for the present and Ref. 5 experiments.

	Pulsejet	Ref. 5 (Resonance Tube)
Formation No.	21.9	3.6
$\eta_m(D/d_j \approx 3.1)$	0.43	1.15
$\eta_m(D/d_j \approx 2.3)$	0.52	1.00

related to the size of the jet source but not the particular structure of the jet.

Since Formation number seems to affect the features of a starting vortex, it may be supposed that it could be used as a parameter to explain the performance differences between the present and Ref. 5 experiments. The Formation number (which is essentially an inverse Strouhal number) may be written as follows.

$$F = \frac{\sqrt{u'^2}}{2fd_j} \quad (11)$$

where f is the frequency of the primary source. Table 3 shows the values obtained for the two experiments. Also listed in the table are values of efficiency derived from the equation

$$\phi_{us} = (1 + \beta_{us})^{\frac{\eta_m}{2}} \quad (12)$$

using the nominal diameter ejector to jet diameter ratios yielding the highest performance in Fig. 12. These quantities are also shown plotted in Fig. 13. It is clear that efficiencies greater than 1.0 are inconsistent; however, it is striking that the high efficiency occurs

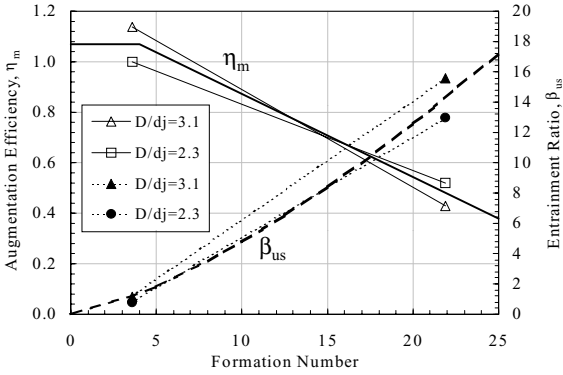


Fig. 13 Unsteady augmentation efficiency and entrainment ratio as functions of Formation number.

precisely at the critical Formation number identified in Ref. 13 as marking the transition from starting vortices without to those with ‘trailing jets’.

Figure 13 also shows some simple curves representing proposed behavior of η_m and β_{us} over the range of Formation numbers. These have no theoretical basis (though arguments can be made for the shape) and are obviously based on extremely limited data. Furthermore, there is no accounting for the temperature of the unsteady flow, which is clearly influential for steady ejectors. Nevertheless, it may be instructive to use these curves in order to obtain unsteady thrust augmentation as a function of Formation number. This is shown in Fig. 14. Also shown are the data from the present and Ref. 5 experiments, from which the curve was constructed, and a single datum from the Ref. 2 experiment. Though the uncertainty in the F is large for this latter point, the agreement with the present curve seems at least encouraging.

It is interesting to consider some of the other results of the present experiment in light of Fig. 14. In particular, it was noted that the pulsejet with the STRAIGHT tailpiece yielded higher thrust augmentation than that with the ORIGINAL flared tailpiece. It was also noted that the STRAIGHT pulsejet had a higher frequency. It has been observed that for the ORIGINAL tailpiece $\sqrt{u'^2}/\bar{u}$ is nearly identical to $\sqrt{\Delta p_{cc}'^2}/\Delta \bar{p}_{cc}$, where Δp_{cc} is the difference between the combustion chamber and ambient pressures. The quantity $\sqrt{u'^2}/\bar{u}$ was not measured for the STRAIGHT tailpiece, nor was the mass flow rate; however, the thrust was measured, as was $\sqrt{\Delta p_{cc}'^2}/\Delta \bar{p}_{cc}$. Assuming the same relationship exists between rms quantities in the STRAIGHT

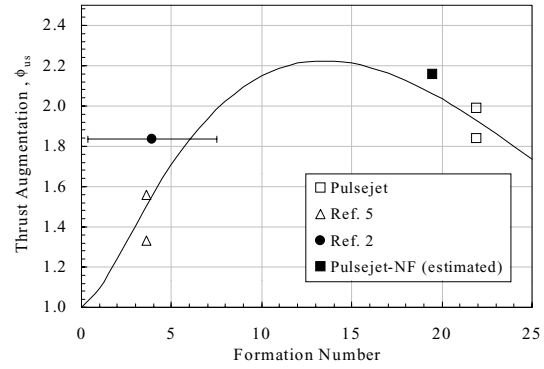


Fig. 14 Unsteady thrust augmentation as a function of Formation number.

Table 4 RMS velocity and Formation number for ideal and experimental PDE's.

	RMS Velocity $\sqrt{u'^2}/\bar{u}$	Formation No. $\frac{\sqrt{u'^2}}{2fd_j}$
Ideal	1.21	21.0
Ref. 14	3.04	110
Ref. 15	0.82	53

pulsejet as those in the ORIGINAL, Eq. 9 can be used (after rearranging) to yield the mass flow rate. This can, in turn be used to find \bar{u} , and ultimately F . The value of ϕ_{us} can also be found allowing an estimated data point to be plotted in Fig. 14 for the STRAIGHT configuration. It can be seen that this point is consistent with predictions made using the model described above.

It is also interesting to consider the implications of the present model with respect to PDE's. It is noted that, in principle, PDE's have a significant thrust component due to unsteady pressure forces. Thus, Eqs. 5, and 6 are no longer valid. Furthermore, the powerful emitted shock from a PDE cycle may have profound effects on ejector performance. Nevertheless, Table 4 shows values of rms velocity and Formation number for an ideal PDE cycle¹¹ and two existing PDE experiments.^{14,15} For the ideal cycle, an assumed $L/d_j=10$ has been used. These results were obtained from 1-D CFD simulations; however, the simulation results agree well with experimental data in terms of thrust produced.

It can be seen from Table 4 that results obtained from current PDE experiments may not be applicable to one that is optimized (e.g. self-aspirating at the maximum

theoretical frequency). The Ref. 14 experiment would apparently exhibit a strong unsteady component of thrust augmentation; however, due to the high Formation number (and extremely high temperature), the unsteady augmentation would be poor. The Ref. 15 experiment would have a relatively weak unsteady augmentation component which would also be poor.

Summary

Thrust augmentation and mass entrainment measurements were presented from an experiment using a series of cylindrical ejectors driven by a pulsejet. Several jet shapes were tested as well. Significant augmentation and entrainment values were obtained compared to similarly sized steady ejectors. Significant observations included the following:

- Optimal ejector length does not scale with ejector diameter.
- The size of the ejector inlet radius can have a strong effect on augmentation.
- For the ejector geometry yielding the highest thrust augmentation, peak values were found when the primary source was in close proximity to the ejector inlet face. Higher values may be possible with the source placed some distance inside the ejector.
- Mass entrainment and thrust augmentation are not monotonically related.

The results were compared to those from an experiment using the same ejectors, but with a primary jet driven by a resonance-tube. A modeling approach that separates the augmentation into steady and unsteady components, weights the components using rms velocity, then determines the unsteady entrainment and augmentation efficiency as functions of Formation number appears to reconcile the observed differences between the experiments. Although far from complete, the modeling approach at least demonstrates the importance of rms velocity and Formation number in determining unsteady ejector performance, and shows how these numbers may be determined from readily obtainable experimental data.

References

1. Lockwood, R.M. "Interim Summary Report on Investigation of the Process of Energy Transfer from an Intermittent Jet to Secondary Fluid in an Ejector-Type Thrust Augmenter," Hiller Aircraft Report No. ARD-286, March, 1961.

2. Binder, G. and Didelle, H, "Improvement of Ejector Thrust Augmentation by pulsating or flapping Jets," Paper E3 of Proc. 2nd Symposium on Jet Pumps & Ejectors and Gas Lift Techniques, Cambridge, England, March 1975.
3. Porter, J.L., and Squyers, R.A., "A Summary/Overview of Ejector Augmentor Theory and Performance Phase II—Technical Report," ATC Report No. R-91100/9CR-47A, Sept., 1979.
4. Kentfield, J.A.C, Nonsteady, One-Dimensional, Internal, Compressible Flows, Oxford University Press, 1993.
5. Wilson, J, and Paxson, D.E., "Unsteady Ejector Performance: An Experimental Investigation Using a Resonance Tube Driver," AIAA paper # 2002-3632.
6. Heiser, W.H., "Thrust Augmentation," ASME paper 66-GT-116, March, 1966.
7. Foa, J.V. Elements of Flight Propulsion, John Wiley and Sons, 1960.
8. Johnson, W.S. and Yang, T. "A Mathematical Model for the Prediction of the induced Flow in a Pulsejet Ejector with Experimental Verification," ASME Paper 68-WA/FE-33, 1968.
9. Marzouk, E.M., and Abdel Wahab, A.F., "A Numerical Model for Prediction of the Induced Flow in Pulse Jet Ejector with Experimental Verification," AIAA-97-1016, 1997.
10. Lockwood, R.M. "Investigation of the Process of Energy Transfer from an Intermittent Jet to Secondary Fluid in an Ejector-Type Thrust Augmenter," Hiller Aircraft Report No. APR-64-4, March, 1964.
11. Paxson, D.E., "A Performance Map for Ideal Air Breathing Pulse Detonation Engines," AIAA paper 2001-3465, July, 2001.
12. Wentworth, T.J, Paxson, D.E., Wernet, M.P., "Conditionally Sampled Pulsejet Driven Ejector Flow Field Using DPIV," AIAA paper 2002-3231, June, 2002.
13. Gharib, M., Rambod, E., Shariff, K., "A universal time scale for vortex ring formation," Journal of Fluid Mechanics, Vol. 360, pp. 121-140, 1998.
14. Schauer, F., Stutrud, J., Bradley, R., "Detonation Initiation Studies and Performance Results for Pulsed Detonation Engine Applications" AIAA Paper 2001-1129, January, 2001.
15. Wolter, J., NASA GRC PDE Rig Data, personal consultations, results unpublished.

Appendix 1 Mass Entrainment Extrapolation

Although the description of the entrainment rig given earlier mentions a sealed containment box, in actuality the box contained a small, fixed opening in the side through which ambient air could flow. The purpose of this opening was to prevent excessive vacuum conditions from occurring (which ultimately prevent the pulsejet from operating) when insufficient air is supplied to the box during ejector tests. With this opening it was possible to run entrainment tests with either too much or too little supply air, thus arriving at the appropriate amount more quickly.

Figure A1 shows the supplied mass flow rate as a function of the square root of the box differential pressure (measured relative to the ambient pressure)

$$\Delta P_{\text{Box}} = P_{\text{ambient}} - P_{\text{Box}} \quad (13)$$

for the four ejectors tested. The ejector diameters are shown in the legend. The data for each ejector is well fit with a linear regression, the y-intercept of which is the correct mass flow rate. For all of the ejectors except $D=6.0$ in. it is seen that there are data points representing both excess and insufficient air. The supply system could not provide enough air for this ejector; however, the trend in the data is clear and consistent with the other ejectors tested. Therefore, extrapolation is warranted and the result may be obtained with confidence.

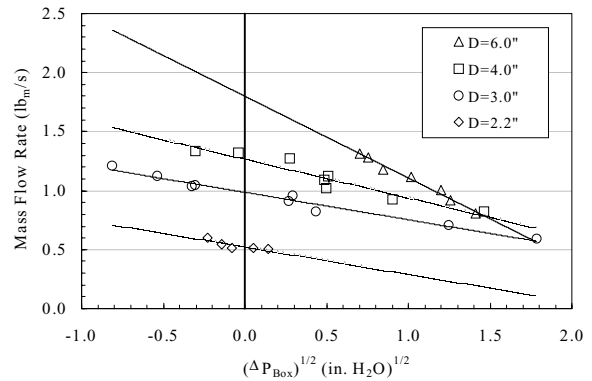


Fig. A1 Containment box mass flow rate as a function of the square root of the box differential pressure for the four ejectors tested.

REPORT DOCUMENTATION PAGE			<i>Form Approved</i> <i>OMB No. 0704-0188</i>	
Public reporting burden for this collection of information is estimated to average 1 hour per response, including the time for reviewing instructions, searching existing data sources, gathering and maintaining the data needed, and completing and reviewing the collection of information. Send comments regarding this burden estimate or any other aspect of this collection of information, including suggestions for reducing this burden, to Washington Headquarters Services, Directorate for Information Operations and Reports, 1215 Jefferson Davis Highway, Suite 1204, Arlington, VA 22202-4302, and to the Office of Management and Budget, Paperwork Reduction Project (0704-0188), Washington, DC 20503.				
1. AGENCY USE ONLY (<i>Leave blank</i>)	2. REPORT DATE June 2002	3. REPORT TYPE AND DATES COVERED Technical Memorandum		
4. TITLE AND SUBTITLE Unsteady Ejector Performance: An Experimental Investigation Using a Pulsejet Driver			5. FUNDING NUMBERS WU-708-48-13-00	
6. AUTHOR(S) Daniel E. Paxson, Jack Wilson, and Kevin T. Dougherty				
7. PERFORMING ORGANIZATION NAME(S) AND ADDRESS(ES) National Aeronautics and Space Administration John H. Glenn Research Center at Lewis Field Cleveland, Ohio 44135-3191			8. PERFORMING ORGANIZATION REPORT NUMBER E-13462	
9. SPONSORING/MONITORING AGENCY NAME(S) AND ADDRESS(ES) National Aeronautics and Space Administration Washington, DC 20546-0001			10. SPONSORING/MONITORING AGENCY REPORT NUMBER NASA TM-2002-211711 AIAA-2002-3915	
11. SUPPLEMENTARY NOTES Prepared for the 38th Joint Propulsion Meeting and Exhibit cosponsored by AIAA, ASME, SAE, and ASEE, Indianapolis, Indiana, July 7-10, 2002. Daniel E. Paxson, NASA Glenn Research Center; Jack Wilson and Kevin T. Dougherty, QSS Group, Inc., Cleveland, Ohio 44135. Responsible person, Daniel E. Paxson, organization code 5530, 216-433-8334.				
12a. DISTRIBUTION/AVAILABILITY STATEMENT Unclassified - Unlimited Subject Category: 07 Available electronically at http://gltrs.grc.nasa.gov/GLTRS This publication is available from the NASA Center for AeroSpace Information, 301-621-0390.			12b. DISTRIBUTION CODE	
13. ABSTRACT (<i>Maximum 200 words</i>) An experimental investigation is described in which thrust augmentation and mass entrainment were measured for a variety of simple cylindrical ejectors driven by a gasoline-fueled pulsejet. The ejectors were of varying length, diameter, and inlet radius. Measurements were also taken to determine the effect on performance of the distance between pulsejet exit and ejector inlet. Limited tests were also conducted to determine the effect of driver cross-sectional shape. Optimal values were found for all three ejector parameters with respect to thrust augmentation. This was not the case with mass entrainment, which increased monotonically with ejector diameter. Thus, it was found that thrust augmentation is not necessarily directly related to mass entrainment, as is often supposed for ejectors. Peak thrust augmentation values of 1.8 were obtained. Peak mass entrainment values of 30 times the driver mass flow were also observed. Details of the experimental setup and results are presented. Preliminary analysis of the results indicates that the enhanced performance obtained with an unsteady jet (primary source) over comparably sized ejectors driven with steady jets is due primarily to the structure of the starting vortex-type flow associated with the former.				
14. SUBJECT TERMS Pulsejet engines; Thrust augmentation; Ejectors			15. NUMBER OF PAGES 19	
			16. PRICE CODE	
17. SECURITY CLASSIFICATION OF REPORT Unclassified	18. SECURITY CLASSIFICATION OF THIS PAGE Unclassified	19. SECURITY CLASSIFICATION OF ABSTRACT Unclassified	20. LIMITATION OF ABSTRACT	